

**Supporting Information for
Controlled crystallisation of porous crystals of luminescent
platinum(II) complexes by electronic tuning of ancillary ligands**

Takanari Mochizuki,^a Masaki Yoshida,^{*b} Atsushi Kobayashi^a and Masako Kato^{*b}

^a Department of Chemistry, Faculty of Science, Hokkaido University
North-10 West-8, Kita-ku, Sapporo, Hokkaido 060-0810, Japan.

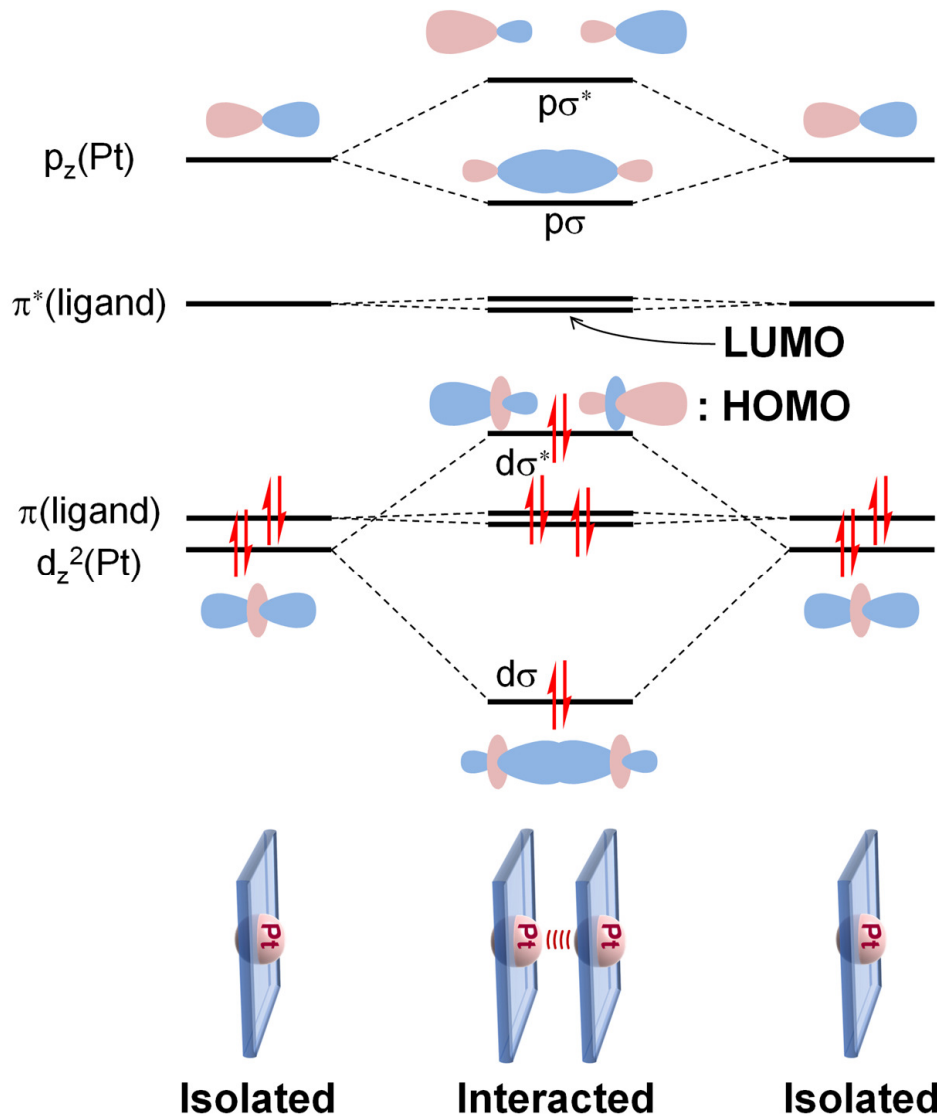
^b Department of Applied Chemistry for Environment, School of Biological and Environmental Sciences, Kwansei Gakuin University
1 Gakuen-Uegahara, Sanda, Hyogo 669-1330, Japan.

E-mail: masaki.yoshida@kwansei.ac.jp, katom@kwansei.ac.jp

Table of Contents

- Scheme S1** Schematic MO energy level diagram for Pt(II) complexes with the Pt \cdots Pt interaction.
- Figs. S1-2** Packing structures of **Pt-pz**, **Pt-Fpy**, and **Pt-py**.
- Fig. S3** Permanent porosity of **Pt-pz**.
- Fig. S4** PXRD patterns of the as-synthesised and the recrystallised **Pt-Fpy**.
- Fig. S5** Stacking structures of **Pt-pz**, **Pt-Fpy**, **Pt-py**, and **Pt-ox**.
- Fig. S6** TG curves of **Pt-pz**, **Pt-Fpy**, and **Pt-py**.
- Figs. S7-S8** Kohn-Sham orbitals and energy diagrams at the frontier region.
- Fig. S9** Absorption spectra in methanol.
- Figs. S10-S11** TDDFT results.
- Figs. S12-S13** NMR spectra of **Pt-pz**, **Pt-Fpy**, and **Pt-ox**.
- Table S1** Crystal parameters and refinement data.
- Table S2** Selected interatomic distances and angles.
- Tables S3-S6** Cartesian coordinates for the optimised structures.
- Tables S7-S8** Computed vertical excitations.

References



Scheme S1 Schematic MO energy level diagram for Pt(II) complexes with appropriate aromatic ligands showing effective Pt…Pt interaction by stacking.

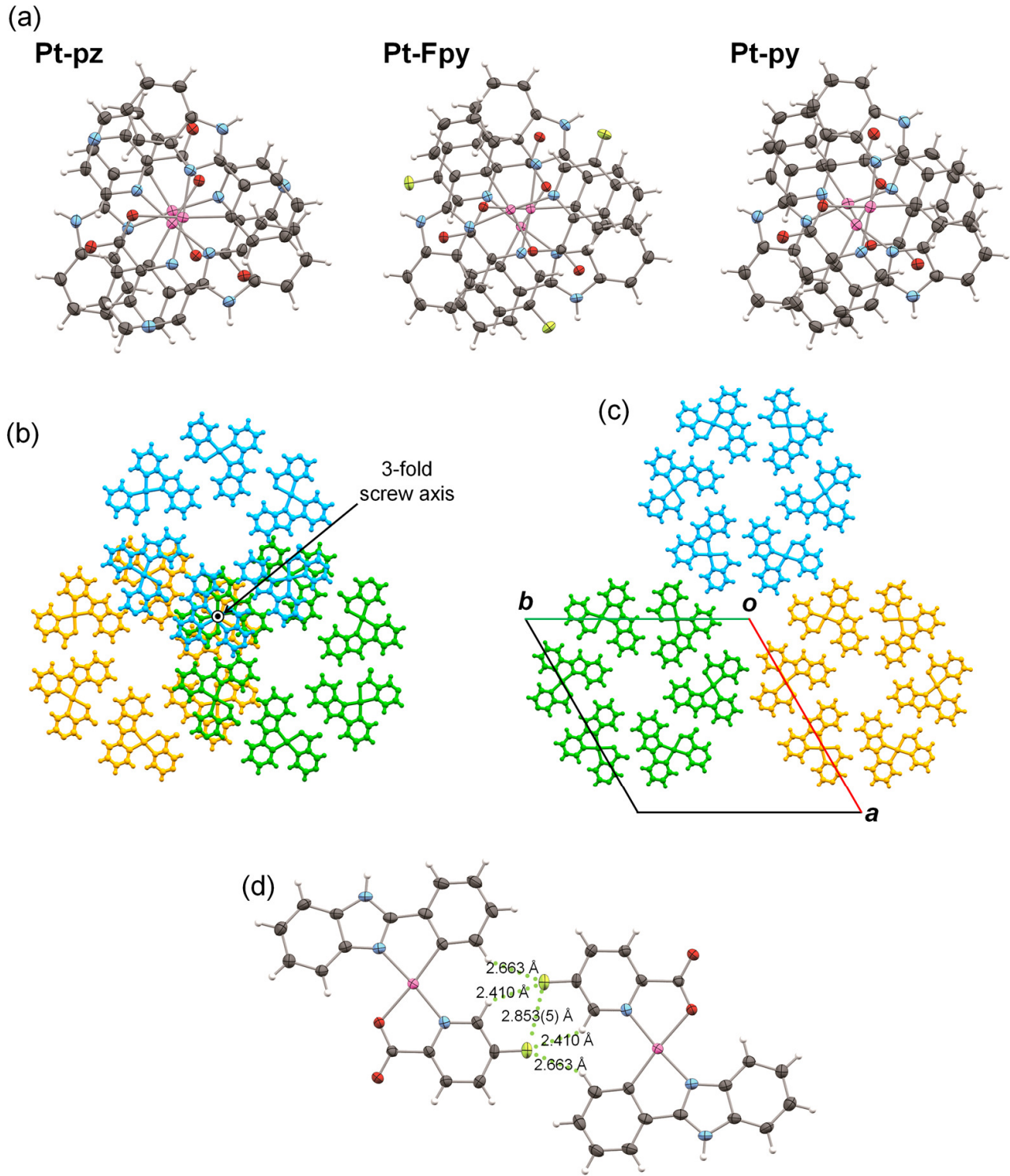


Fig. S1 (a) Stacking structures of **Pt-pz**, **Pt-Fpy**, and **Pt-py** (cyclohexane-included form)^{S1} viewed along the *c*-axis. (b) Stacking structure of the cyclic hexamer **Pt-pz** along a 3-fold screw axis. (c) Two-dimensional sheet structure of **Pt-pz**. For (b) and (c), each hydrogen-bonded cyclic hexamer is drawn in a different colour for clarity. (d) F···F and CH···F interactions between **Pt-Fpy** in the *ab*-plane.

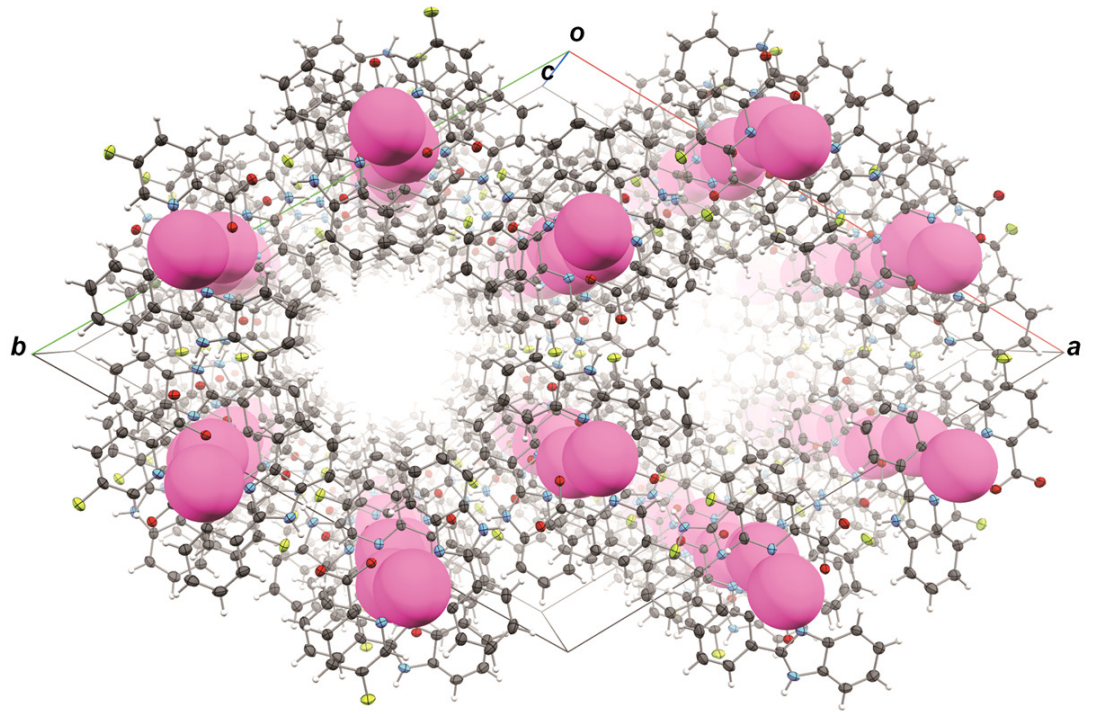


Fig. S2 Porous structure of **Pt-Fpy**. Thermal ellipsoids are displayed at the 50% probability level. For clarity, Pt atoms are shown with a space-filling model.

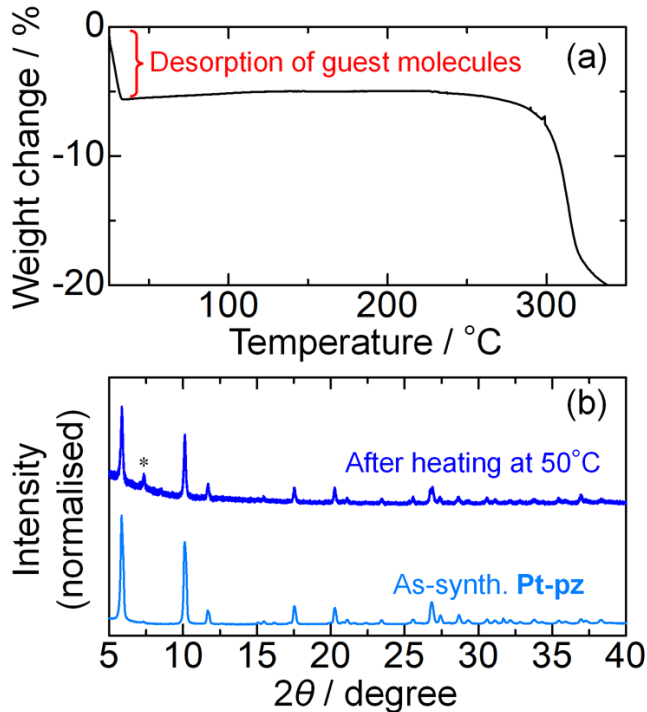


Fig. S3 (a) TG curve of as-synthesised **Pt-pz** (scan rate = $1\text{ }^{\circ}\text{C min}^{-1}$). This sample showed a weight loss of about 5.6% by $35\text{ }^{\circ}\text{C}$, attributable to the desorption of guest molecules in the pores. (b) PXRD patterns of **Pt-pz** before and after the desorption of guest molecules by heating at $50\text{ }^{\circ}\text{C}$ (the peak indicated with an asterisk (*) is an artifact from the sample holder). Each peak position of the PXRD pattern of **Pt-pz** remained unchanged after the desorption of the guest molecules, indicating the permanent porosity. Such permanent porosity was also observed for **Pt-py**.^{S1}

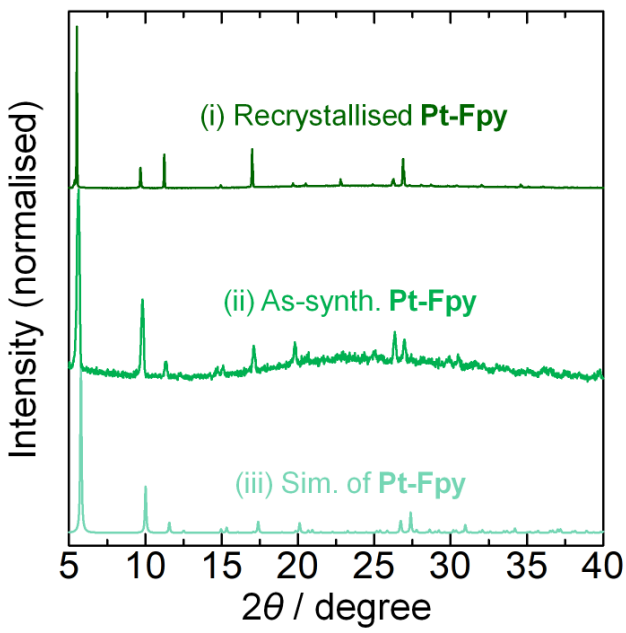


Fig. S4 PXRD patterns of (i) recrystallised and (ii) as-synthesised samples of **Pt-Fpy**, as well as the (iii) simulated PXRD pattern based on the single crystal X-ray structure of **Pt-Fpy**. The recrystallisation was achieved through the slow diffusion of $^t\text{BuOMe}$ vapour into the DMF solution of **Pt-Fpy**. The PXRD pattern of the as-synthesised sample clearly showed an amorphous halo at around 20-30°, whereas the pattern of the recrystallised sample displayed no halo and sharp peaks, indicating the absence of the amorphous component after the recrystallisation.

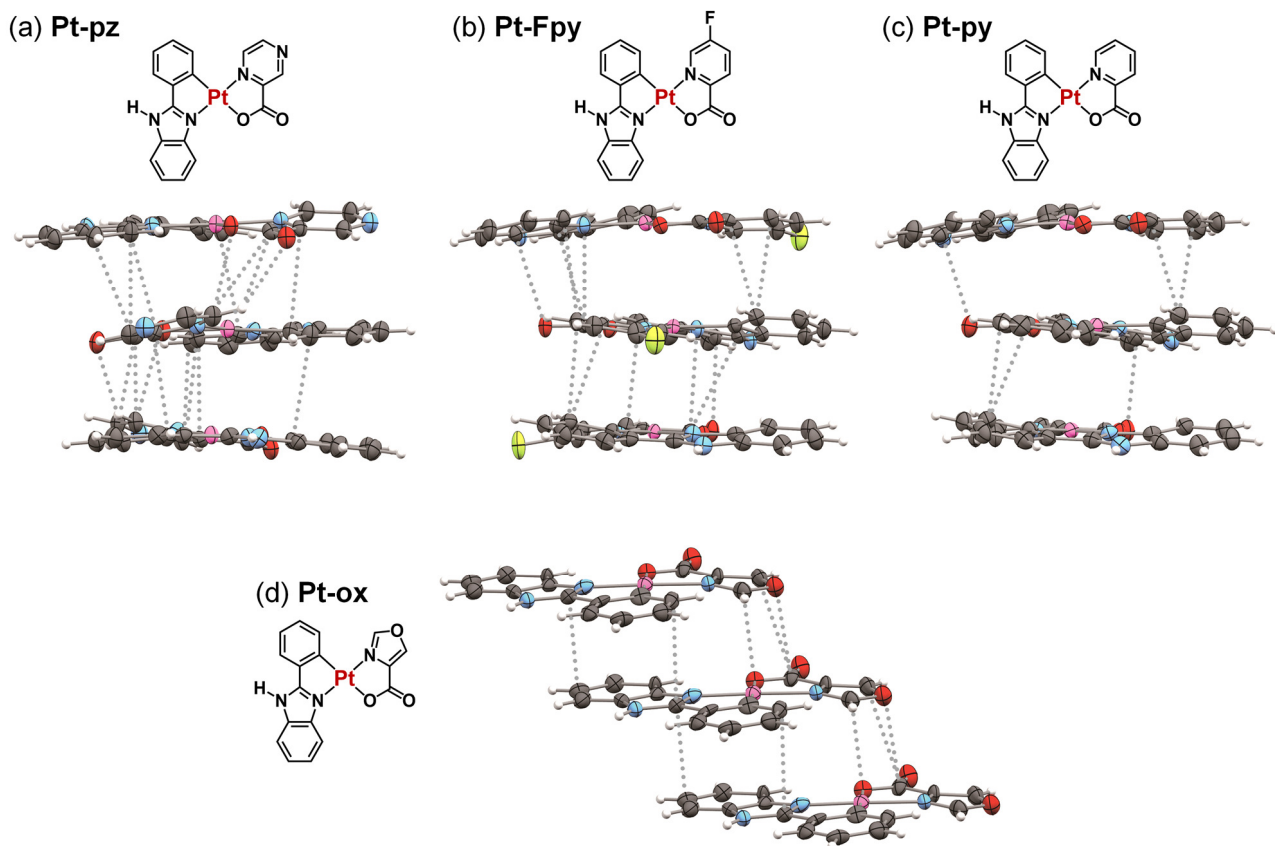


Fig. S5 Stacking structures of (a) **Pt-pz**, (b) **Pt-Fpy**, (c) **Pt-py** (cyclohexane-included form),^{S1} and (d) **Pt-ox**. The grey dotted lines indicate pairs of atoms in the ligand for which the interatomic distance is shorter than the sum of the van der Waals radii.

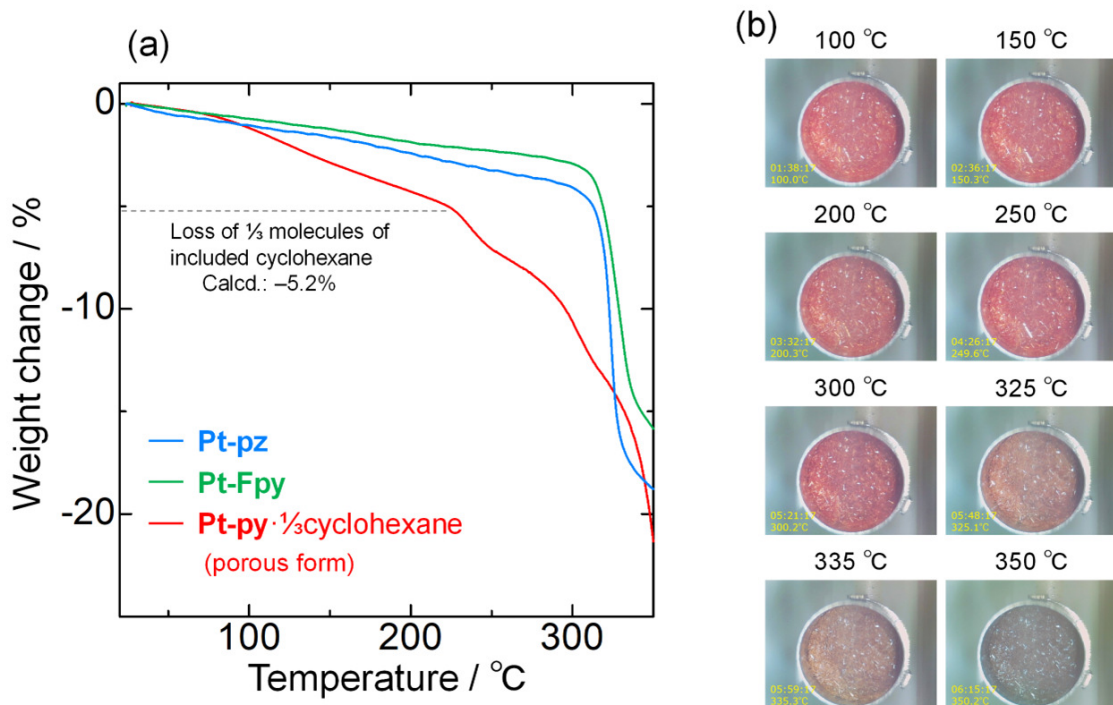


Fig. S6 (a) TG curves of recrystallised samples of **Pt-pz** (blue), **Pt-Fpy** (green), and **Pt-py** (cyclohexane-included porous form; red),^{S1} and (b) the photographs of **Pt-Fpy** during the TG analysis (scan rate = 1 °C min⁻¹).

As the samples of **Pt-pz** and **Pt-Fpy** were air-dried before measurement, no significant desorption of guest molecules was observed, in contrast to Fig. S3(a). Decomposition temperatures of **Pt-pz** and **Pt-Fpy** were estimated to be approximately 318 and 316 °C, respectively. The decomposition of **Pt-Fpy** above ca. 316 °C was further confirmed by the photographs taken at each temperature.

For **Pt-py**, after the desorption of included cyclohexane molecules,^{S1} a gradual weight loss assignable to the decomposition was observed above ca. 225 °C. This decomposition temperature is significantly lower than those of **Pt-pz** (ca. 318 °C) and **Pt-Fpy** (ca. 316 °C), suggesting the weaker intermolecular interactions in **Pt-py**.

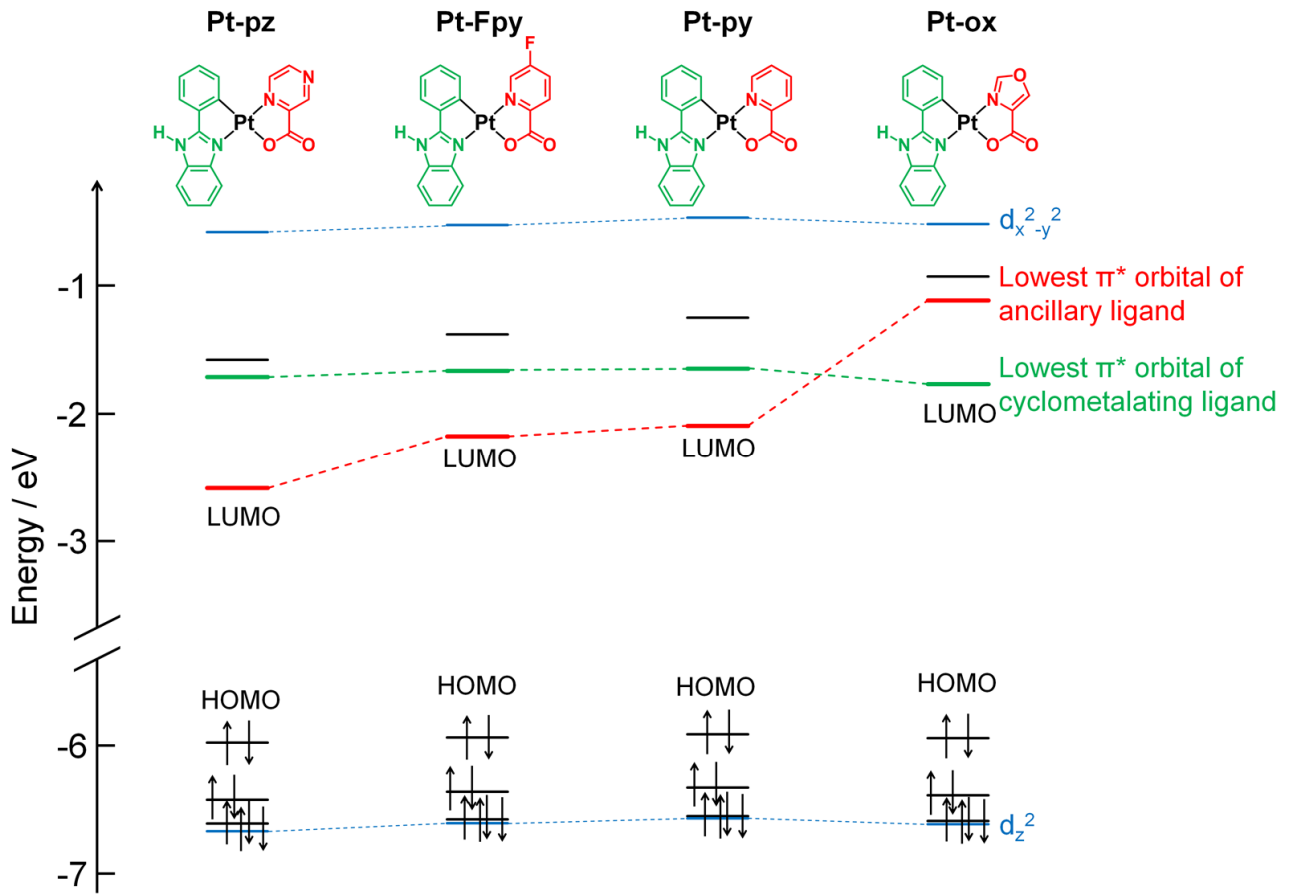


Fig. S7 Energy level diagrams for the optimised singlet ground state of **Pt-pz**, **Pt-Fpy**, **Pt-py**, and **Pt-ox**, where the Kohn-Sham orbitals of complexes are summarised in Fig. S8(a-d). In **Pt-pz**, the lowest π^* orbital of the ancillary ligand appears to be a LUMO. Among these complexes, **Pt-pz** has the lowest energy for the lowest π^* orbital of the ancillary ligand (-2.584 eV), followed by **Pt-Fpy** (-2.179 eV) and **Pt-py** (-2.090 eV). In **Pt-ox**, the lowest π^* orbital of the ancillary ligand (-1.117 eV) has a higher energy than the lowest π^* orbital of the cyclometalating ligand. Thus, among these complexes, the pyrazyl group of pyrazinecarboxylate in **Pt-pz** was suggested to have the most δ^+ nature.

In addition, there were no significant changes observed in the energies of the occupied d_z^2 orbitals and unoccupied $d_{x^2-y^2}^2$ orbitals among the complexes. This suggests that the ligand field strength is not significantly different between them.

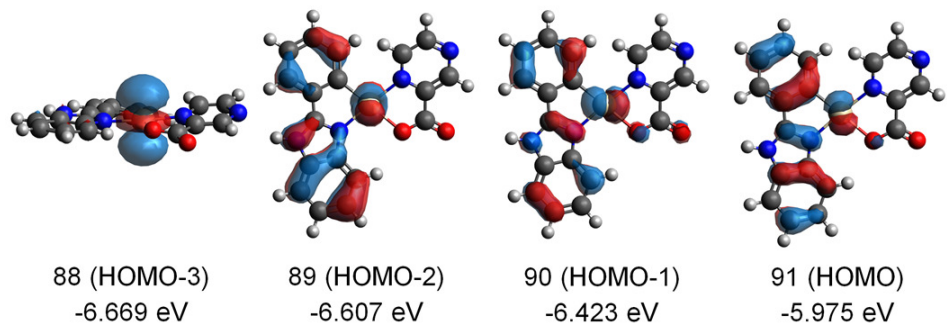
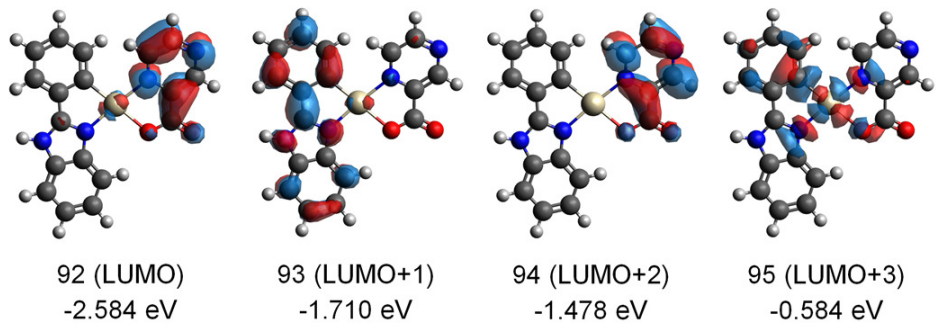


Fig. S8(a) Kohn–Sham orbitals in the frontier region for the singlet ground state of **Pt-pz** (isovalue = 0.035) with their energies (eV).

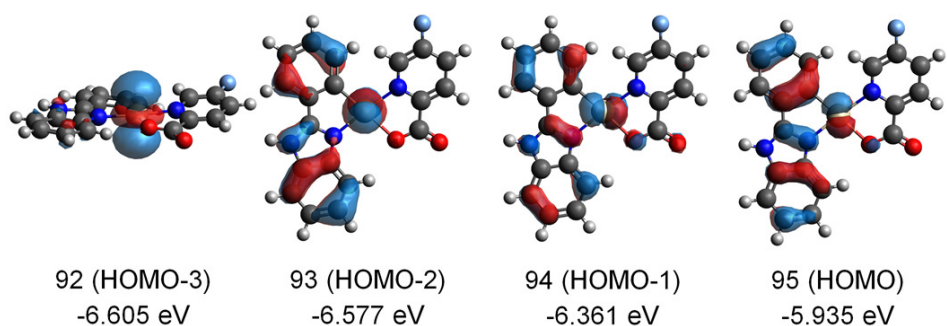
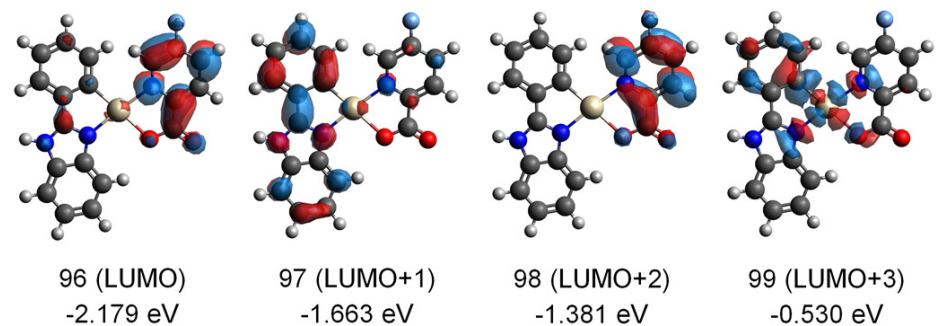


Fig. S8(b) Kohn–Sham orbitals in the frontier region for the singlet ground state of **Pt-Fpy** (isovalue = 0.035) with their energies (eV).

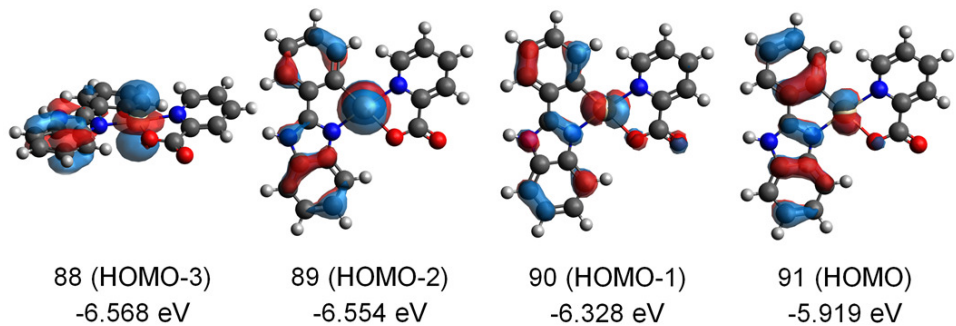
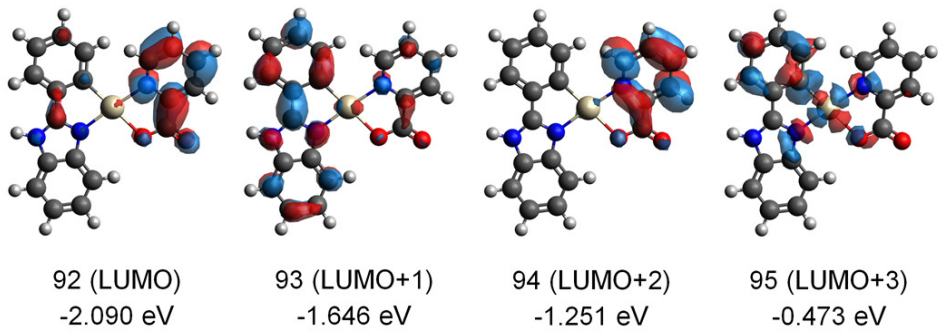


Fig. S8(c) Kohn–Sham orbitals in the frontier region for the singlet ground state of **Pt-py** (isovalue = 0.035) with their energies (eV).

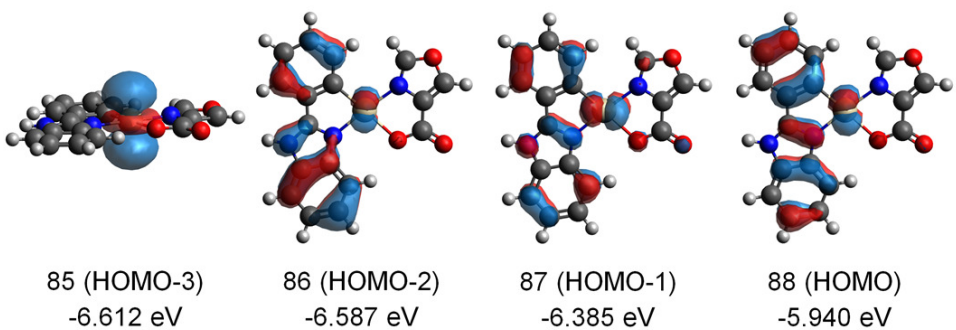
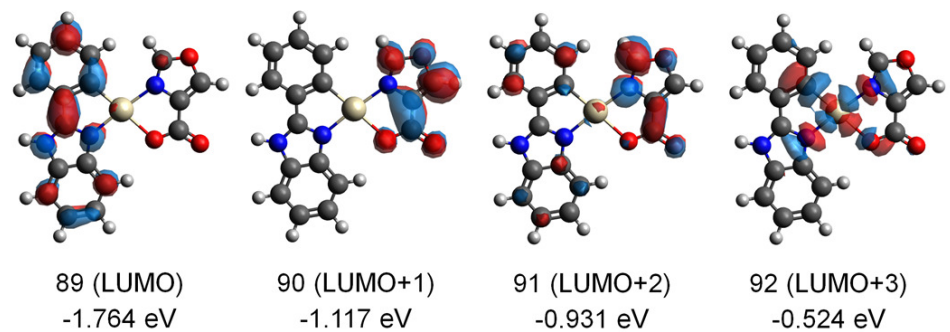


Fig. S8(d) Kohn–Sham orbitals in the frontier region for the singlet ground state of **Pt-ox** (isovalue = 0.035) with their energies (eV).

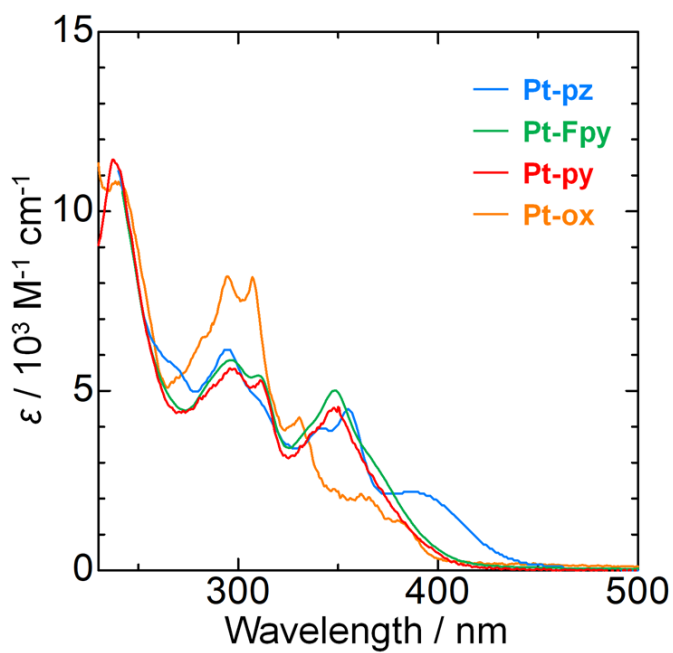


Fig. S9 UV-vis absorption spectra of **Pt-pz** (blue), **Pt-Fpy** (green), **Pt-ox** (orange), and **Pt-py** (red) in methanol solution ($c = 2.0 \times 10^{-5} \text{ M}$).

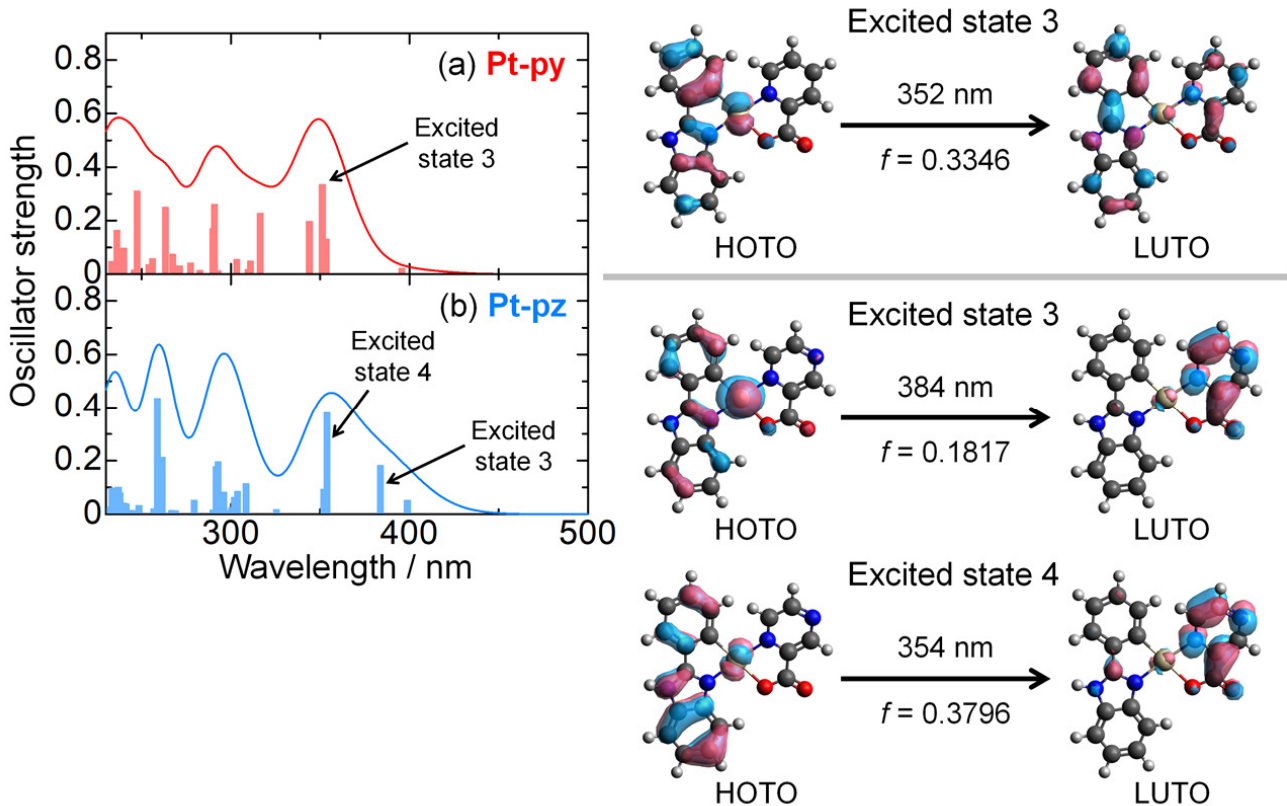


Fig. S10 The calculated singlet excitations (vertical bars), simulated absorption spectra, and natural transition orbitals (NTOs) for the important vertical excitations of (a) **Pt-py** and (b) **Pt-pz**. The highest occupied transition orbital (HOTO) and the lowest unoccupied transition orbital (LUTO) indicate the occupied “hole” and the unoccupied “electron”, respectively. To obtain the simulated absorption spectra, transition energies and oscillator strengths have been interpolated by a Gaussian convolution with a common σ value of 0.15 eV.

Notably, as shown in Fig. S9, only **Pt-pz** exhibited a moderate absorption peak at 386 nm among the current compounds. This feature is well reproduced by the TDDFT calculation. According to the TDDFT result, the moderate absorption shoulder at longer wavelength region is mainly due to $^1\text{MLCT}$ transition (excited state 3, $\lambda = 384$ nm), while the strong absorption peak around 350 nm is due to the singlet mixed metal-ligand-to-ligand charge transfer-type transition (excited state 4, $\lambda = 354$ nm).

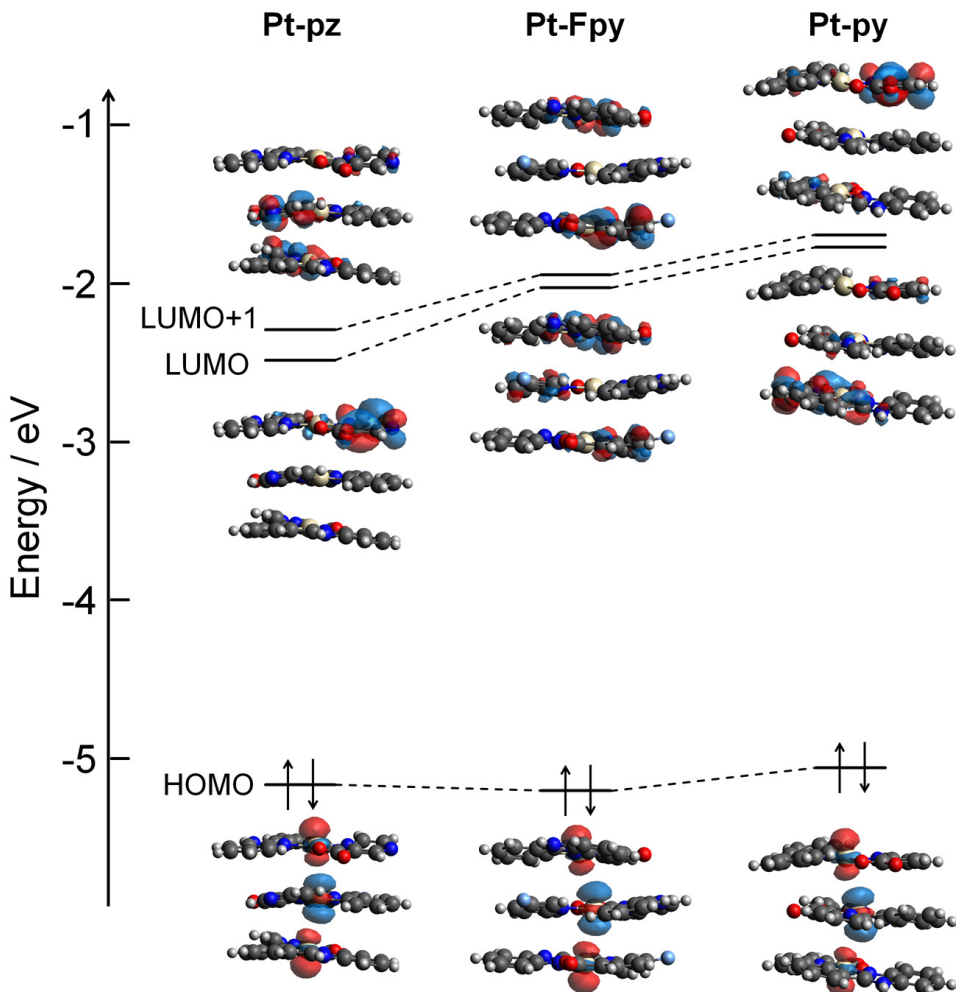


Fig. S11 Khon-Sham orbitals at the frontier region of the trimeric fragments of **Pt-pz**, **Pt-Fpy**, and **Pt-py** (isovalue = 0.035). HOMO is mainly localised on the $d\sigma^*$ orbital between Pt atoms, while LUMO and LUMO+1 are delocalised on the π^* orbitals of the ligands. Thus, the HOMO-LUMO transitions in these systems should be assigned to the $d\sigma^*\rightarrow\pi^*$ (i.e., MMLCT) transitions.

Although the HOMO energy of **Pt-pz** is expected to be the most destabilised because the $d\sigma^*$ should be destabilised as the $\text{Pt}\cdots\text{Pt}$ distance decreases (Scheme S1), the calculation results showed no significant difference in energy between the three complexes. This might be because no molecular structure optimisation was performed in the present calculations, and only three molecules of the one-dimensional $\text{Pt}\cdots\text{Pt}$ chain were used to calculate the electronic structure.

On the other hand, the calculation results showed that the HOMO-LUMO gap is also affected by the energy of the LUMO (i.e. the pyrazine, fluoropyridine and pyridine moieties on the auxiliary ligand). Thus, the HOMO-LUMO gap is smallest for **Pt-pz**, followed by **Pt-Fpy** and **Pt-py**.

Supplementary NMR spectra for characterisations.

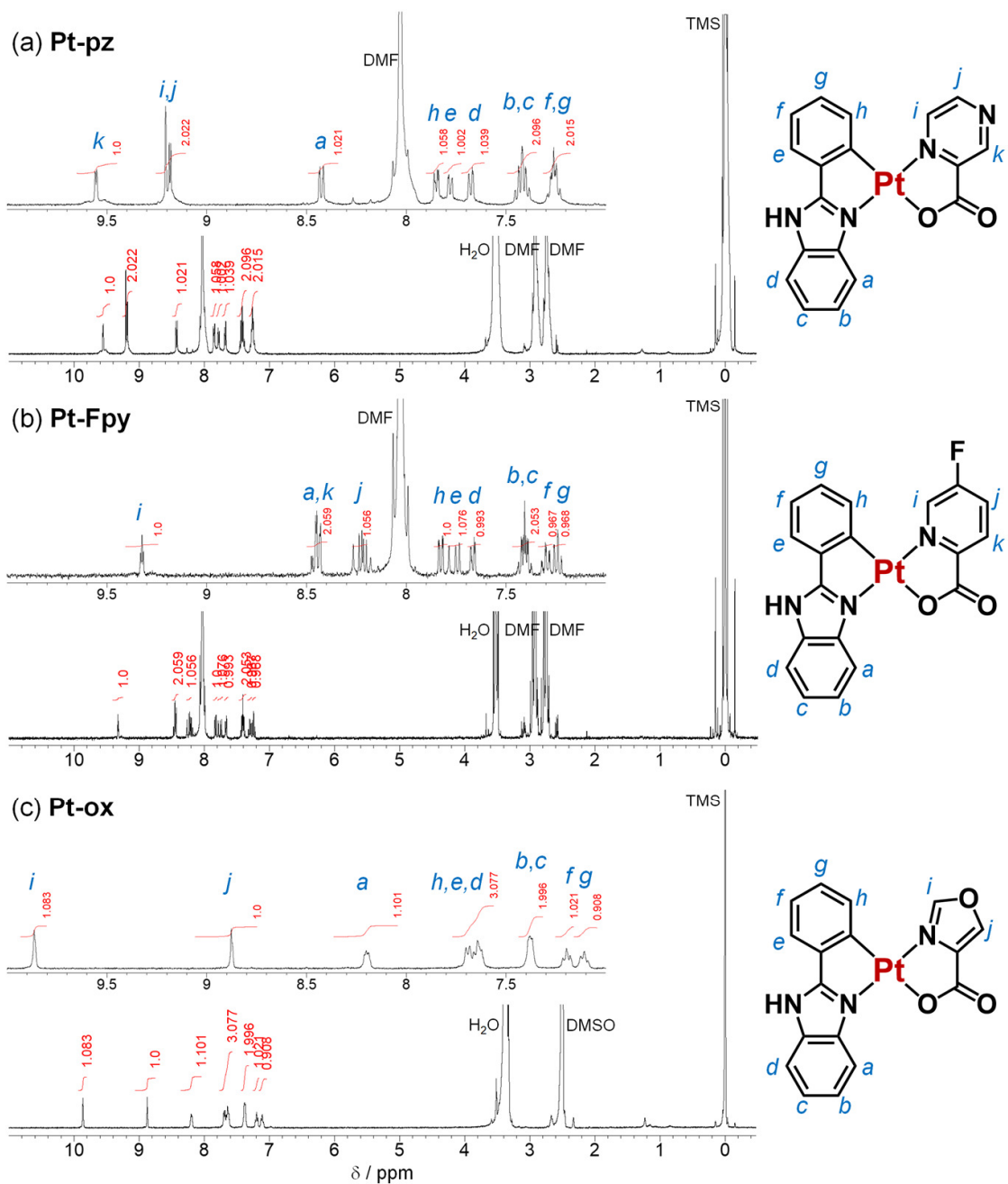


Fig. S12 ^1H NMR spectra (400 MHz) of (a) **Pt-pz**, (b) **Pt-Fpy**, and (c) **Pt-ox** in $\text{DMF}-d_7$ (for **Pt-Fpy** and **Pt-pz**) or $\text{DMSO}-d_6$ (**Pt-ox**) at 298 K. Since a slight ligand dissociation was observed for **Pt-Fpy** and **Pt-pz** in DMSO, $\text{DMF}-d_7$ was used instead of $\text{DMSO}-d_6$ as the solvent for the measurements.

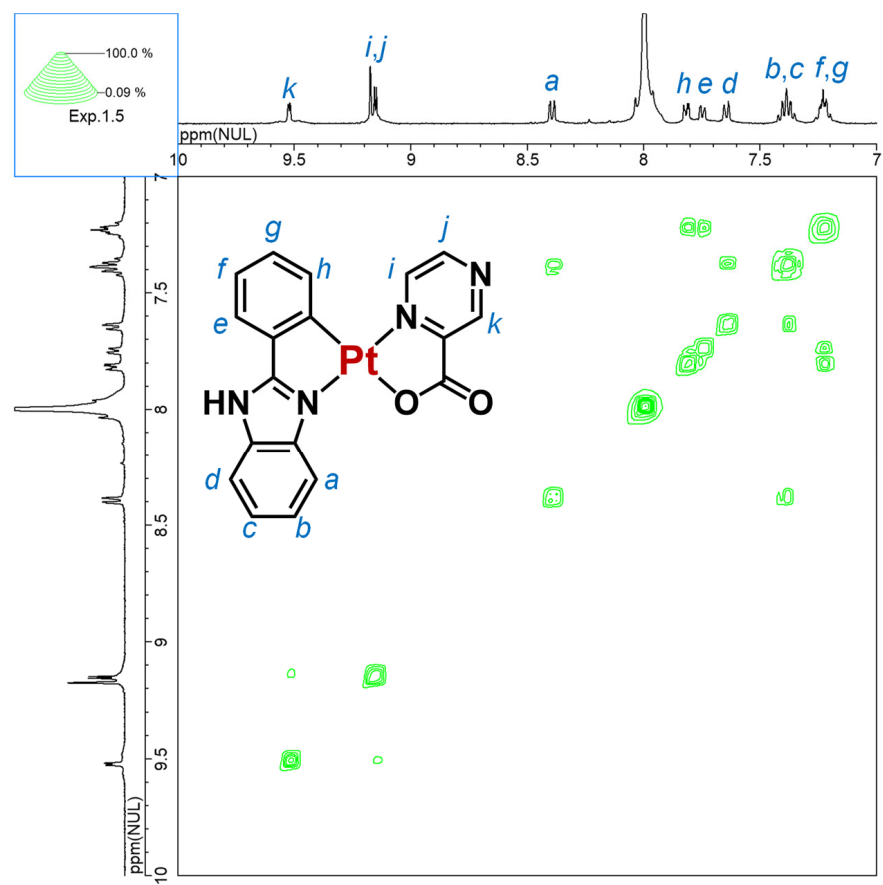


Fig. S13 ^1H - ^1H COSY NMR spectrum (400 MHz) of Pt-pz in $\text{DMF}-d_7$ at 298 K.

Supplementary Tables for X-ray crystallography and DFT calculation

Table S1 Crystal parameters and refinement data.

	Pt-pz	Pt-Fpy	Pt-ox
Formula	C ₁₈ H ₁₂ N ₄ O ₂ Pt [+ solvent]	C ₁₉ H ₁₂ FN ₃ O ₂ Pt [+ solvent]	C ₁₇ H ₁₁ N ₃ O ₃ Pt
Formula weight	511.41	528.41	500.38
Crystal system	Trigonal	Trigonal	Orthorhombic
Space group	R $\bar{3}$ (#148)	R $\bar{3}$ (#148)	P2 ₁ 2 ₁ 2 ₁ (#19)
<i>a</i> / Å	30.2788(4)	30.568(1)	18.7698(5)
<i>b</i> / Å	30.2788(4)	30.568(1)	15.2043(3)
<i>c</i> / Å	9.8954(1)	9.9905(4)	5.0653(1)
α / deg	90	90	90
β / deg	90	90	90
γ / deg	120	120	90
<i>V</i> / Å ³	7856.7(2)	8084.6(6)	1445.54(6)
<i>Z</i>	18	18	4
<i>D</i> _{calc} / g cm ⁻¹	1.946	1.954	2.299
<i>T</i> / K	150	150	150
Reflns collected	9681	20529	5136
Unique reflns	3482	4582	2700
GOF on <i>F</i> ²	1.124	1.067	1.114
<i>R</i> _{int}	0.0258	0.0622	0.0327
<i>R</i> ₁ (<i>I</i> > 2σ(<i>I</i>)) ^[a]	0.0217	0.0344	0.0500
w <i>R</i> ₂ ^[b]	0.0596	0.0748	0.1485
CCDC No.	2333937	2333938	2333939

[a] $R_1 = \sum ||F_o| - |F_c|| / \sum |F_o|$. [b] $wR_2 = [\sum w(F_o^2 - F_c^2) / \sum w(F_o)^2]^{1/2}$, $w = [\sigma_c^2(F_o^2) + (xP)^2 + yP]^{-1}$, $P = (F_o^2 - 2F_c^2)/3$.

Table S2 Selected interatomic distances (Å) and angles (deg) of complexes.

	Pt-pz	Pt-Fpy	Pt-py^[a]	Pt-ox
Distances / Å				
Pt1-C1	2.018(3)	2.004(4)	2.021(3)	2.00(1)
Pt1-N1	2.002(3)	1.995(4)	1.999(3)	1.97(1)
Pt1-N3	2.029(3)	2.022(3)	2.028(3)	2.048(9)
Pt1-O1	2.123(2)	2.105(3)	2.105(2)	2.130(8)
Pt1-Pt1'	3.3390(3)	3.4503(4)	3.4994(4)	–
Angles / deg				
C1-Pt1-N1	79.8(1)	80.1(2)	80.1(1)	80.2(5)
C1-Pt1-N3	104.3(1)	104.7(2)	104.7(1)	103.1(5)
C1-Pt1-O1	175.1(1)	174.9(1)	175.5(1)	177.2(5)
N1-Pt1-N3	175.7(1)	174.5(1)	174.4(1)	176.0(4)
N1-Pt1-O1	96.6(1)	94.9(1)	95.4(1)	97.1(4)
N3-Pt1-O1	79.3(1)	80.3(1)	79.8(1)	79.7(4)
Pt1'-Pt1-Pt1"	164.53(2)	153.81(2)	151.23(2)	–

[a] Cyclohexane-included form; previously reported in Ref. S1.

Table S3 Cartesian coordinates for the optimised structure of **Pt-pz**.

Atom	x	y	z	Atom	x	y	z
Pt1	0.398291	-0.037576	-0.025913	H20	-5.923704	-3.009873	0.210012
C2	0.013728	1.946935	-0.105918	H21	-6.012124	-0.523261	0.330894
C3	-0.896341	4.640742	-0.194153	N22	-1.633161	-0.064380	-0.013705
C4	0.893045	3.002255	-0.357926	C23	-2.218916	1.133520	0.092113
C5	-1.362436	2.292369	0.027712	N24	-3.558319	0.995126	0.196474
C6	-1.813057	3.612972	0.000195	N25	2.449099	-0.135899	0.143788
C7	0.447168	4.327670	-0.393351	N26	5.191041	-0.622806	0.332914
H8	1.939678	2.816172	-0.558134	C27	2.958478	-1.371989	-0.070614
H9	-2.869692	3.831785	0.112962	C28	3.300532	0.830591	0.509815
H10	1.161744	5.120903	-0.585295	C29	4.664666	0.573360	0.597937
H11	-1.228780	5.671667	-0.215649	C30	4.326294	-1.589182	0.011755
H12	-1.624175	-2.936054	-0.139260	H31	2.896923	1.801451	0.745293
C13	-2.571851	-2.424259	-0.038370	H32	5.339125	1.369273	0.890939
C14	-5.070087	-1.047578	0.229082	H33	4.715085	-2.581240	-0.181257
C15	-2.625587	-1.032152	0.028358	O34	0.743203	-2.174346	-0.141148
C16	-3.778843	-3.110452	0.029492	C35	1.979483	-2.496573	-0.302908
C17	-5.006236	-2.435497	0.160871	O36	2.397899	-3.619582	-0.580860
C18	-3.862484	-0.360292	0.160417	H37	-4.220102	1.755620	0.283479
H19	-3.775453	-4.192989	-0.020004				

Table S4 Cartesian coordinates for the optimised structure of **Pt-Fpy**.

Atom	x	y	z	Atom	x	y	z
Pt1	0.213579	-0.105400	-0.066441	H20	-6.309709	-2.580310	0.354782
C2	-0.019324	1.902716	-0.156447	H21	-6.204125	-0.093499	0.458261
C3	-0.723436	4.659417	-0.245817	N22	-1.813340	0.026063	-0.006161
C4	0.929158	2.887148	-0.444289	C23	-2.302445	1.265678	0.106266
C5	-1.361228	2.354729	0.010529	N24	-3.645777	1.230840	0.247980
C6	-1.709859	3.706061	-0.017219	N25	2.262483	-0.374579	0.058451
C7	0.585811	4.242524	-0.480108	C26	4.964292	-1.065964	0.205755
H8	1.951412	2.619880	-0.675409	C27	2.661051	-1.656378	-0.144268
H9	-2.742526	4.006681	0.124327	C28	3.175729	0.548303	0.385515
H10	1.353315	4.976878	-0.700096	C29	4.518592	0.216506	0.459148
H11	-0.976582	5.712691	-0.266815	C30	3.997585	-2.018052	-0.092422
H12	-2.028742	-2.840078	-0.109653	H31	2.846989	1.550393	0.607704
C13	-2.930691	-2.255381	0.012264	H32	4.261132	-3.050943	-0.272682
C14	-5.308052	-0.689168	0.335830	H33	6.017830	-1.308550	0.260377
C15	-2.875304	-0.862647	0.070140	O34	0.374428	-2.255460	-0.162338
C16	-4.184606	-2.846120	0.117605	C35	1.576256	-2.688463	-0.333373
C17	-5.352699	-2.078205	0.276392	O36	1.879772	-3.853451	-0.590966
C18	-4.053388	-0.097251	0.230116	H37	-4.246046	2.039193	0.345934
H19	-4.265542	-3.926008	0.076458	F38	5.389068	1.184127	0.792225

Table S5 Cartesian coordinates for the optimised structure of **Pt-py**.

Atom	x	y	z	Atom	x	y	z
Pt1	0.396981	-0.041430	-0.012687	H20	-5.937482	-2.996655	0.211492
C2	0.015420	1.943359	-0.103745	H21	-6.021051	-0.509049	0.311991
C3	-0.893278	4.639351	-0.222294	N22	-1.638117	-0.063282	-0.009868
C4	0.896390	2.998351	-0.356457	C23	-2.221251	1.136268	0.083037
C5	-1.361845	2.292670	0.015648	N24	-3.562725	1.002703	0.180302
C6	-1.811582	3.613430	-0.026797	H25	-4.222803	1.765483	0.258171
C7	0.451880	4.323477	-0.406972	N26	2.454367	-0.148129	0.157859
H8	1.944954	2.809965	-0.543660	C27	5.194200	-0.605192	0.310173
H9	-2.869123	3.833531	0.075018	C28	2.962637	-1.382592	-0.088286
H10	1.168645	5.114767	-0.599258	C29	3.289761	0.830957	0.539628
H11	-1.225066	5.670217	-0.255718	C30	4.661704	0.638348	0.623852
H12	-1.635741	-2.934844	-0.113535	C31	4.323327	-1.632340	-0.038399
C13	-2.582909	-2.420307	-0.021737	H32	2.844602	1.778785	0.794373
C14	-5.079488	-1.036099	0.220076	H33	4.673437	-2.632302	-0.254970
C15	-2.633538	-1.027414	0.033752	H34	6.261904	-0.780149	0.356416
C16	-3.791752	-3.103426	0.044488	O35	0.733418	-2.172596	-0.130277
C17	-5.018410	-2.424724	0.163250	C36	1.967048	-2.494766	-0.322717
C18	-3.869988	-0.351828	0.153209	O37	2.365195	-3.618449	-0.630458
H19	-3.790495	-4.186355	0.003616	H38	5.290137	1.462344	0.935266

Table S6 Cartesian coordinates for the optimised structure of **Pt-ox**.

Atom	x	y	z	Atom	x	y	z
Pt1	-0.529768	-0.017013	-0.000026	C19	2.426663	-2.424329	-0.000188
C2	-0.143411	1.963080	-0.000035	H20	5.889352	-0.528499	-0.000039
C3	0.770743	4.657397	0.000187	C21	4.941349	-1.051940	-0.000093
C4	1.241396	2.299824	0.000231	H22	5.786591	-3.018061	-0.000323
C5	-1.039611	3.033728	-0.000268	C23	4.869458	-2.441027	-0.000246
C6	-0.590910	4.358152	-0.000154	H24	3.623743	-4.197321	-0.000390
C7	1.695894	3.619310	0.000350	C25	3.633789	-3.113658	-0.000287
H8	-2.106196	2.862307	-0.000625	N26	-2.591559	-0.121157	-0.000085
H9	-1.318317	5.162952	-0.000336	O27	-4.780615	-0.072091	-0.000263
H10	2.760118	3.830061	0.000570	C28	-3.064831	-1.444167	0.000090
H11	1.106123	5.687603	0.000318	C29	-4.412247	-1.393283	-0.000059
N12	1.498056	-0.058884	0.000086	C30	-3.644608	0.641886	-0.000253
C13	2.094441	1.137910	0.000237	H31	-5.198712	-2.127491	0.000044
C14	2.487942	-1.030673	-0.000065	H32	-3.723079	1.713864	-0.000348
H15	4.106297	1.755178	0.000163	O33	-0.856650	-2.182260	0.000057
N16	3.437664	0.995838	0.000198	C34	-2.088802	-2.565745	0.000272
C17	3.733610	-0.361339	-0.000006	O35	-2.481702	-3.733141	0.000652
H18	1.473373	-2.934986	-0.000210				

Table S7 Computed vertical transitions of Pt-pz.

Excited State	1:	Singlet-A	2.7266 eV	454.73 nm	f=0.0004	<S**2>=0.000
	89 -> 92	0.10078				
	90 -> 92	0.12202				
	91 -> 92	0.68429				
Excited State	2:	Singlet-A	3.1062 eV	399.15 nm	f=0.0521	<S**2>=0.000
	88 -> 92	0.53018				
	89 -> 92	-0.12414				
	90 -> 92	0.44041				
Excited State	3:	Singlet-A	3.2284 eV	384.05 nm	f=0.1817	<S**2>=0.000
	88 -> 92	-0.42067				
	89 -> 92	0.14942				
	90 -> 92	0.52611				
	91 -> 92	-0.11046				
Excited State	4:	Singlet-A	3.5014 eV	354.10 nm	f=0.3796	<S**2>=0.000
	87 -> 92	0.11987				
	88 -> 92	0.13929				
	89 -> 92	0.52220				
	91 -> 93	0.42000				
Excited State	5:	Singlet-A	3.5194 eV	352.29 nm	f=0.0934	<S**2>=0.000
	88 -> 92	-0.12731				
	89 -> 92	-0.39720				
	91 -> 93	0.54937				
Excited State	6:	Singlet-A	3.7547 eV	330.21 nm	f=0.0011	<S**2>=0.000
	82 -> 92	-0.13586				
	86 -> 92	0.62919				
	87 -> 92	-0.22176				
Excited State	7:	Singlet-A	3.8055 eV	325.80 nm	f=0.0168	<S**2>=0.000
	91 -> 94	0.67782				
Excited State	8:	Singlet-A	4.0142 eV	308.86 nm	f=0.1147	<S**2>=0.000

(Continued)

88 -> 93	0.38885
90 -> 93	0.56389
<hr/>	
Excited State 9:	Singlet-A 4.0792 eV 303.94 nm f=0.0847 <S**2>=0.000
84 -> 92	0.18680
86 -> 92	0.16159
87 -> 92	0.50136
88 -> 93	-0.28379
89 -> 93	0.10401
90 -> 93	0.12319
91 -> 95	-0.16593
<hr/>	
Excited State 10:	Singlet-A 4.1022 eV 302.24 nm f=0.0631 <S**2>=0.000
84 -> 92	0.32377
85 -> 92	-0.14314
87 -> 92	0.18145
88 -> 93	0.38679
89 -> 93	-0.16813
90 -> 93	-0.31934
<hr/>	
Excited State 11:	Singlet-A 4.1238 eV 300.66 nm f=0.0251 <S**2>=0.000
84 -> 92	0.41422
85 -> 92	-0.19797
86 -> 92	-0.14500
87 -> 92	-0.30848
90 -> 93	0.10064
91 -> 95	-0.28819
<hr/>	
Excited State 12:	Singlet-A 4.1682 eV 297.45 nm f=0.0120 <S**2>=0.000
82 -> 92	-0.22537
84 -> 92	0.23540
88 -> 93	-0.17568
89 -> 95	0.11691
90 -> 94	0.19966
90 -> 95	0.13695
91 -> 95	0.43952
91 -> 96	0.17871

(Continued)

Excited State	13:	Singlet-A	4.1845 eV	296.29 nm	f=0.0825	<S**2>=0.000
	87 -> 92	0.12125				
	88 -> 94	0.22092				
	89 -> 93	-0.16558				
	90 -> 94	0.57140				
Excited State	14:	Singlet-A	4.2308 eV	293.05 nm	f=0.1961	<S**2>=0.000
	82 -> 92	0.36879				
	83 -> 92	-0.13531				
	85 -> 92	-0.32860				
	86 -> 92	0.15104				
	89 -> 93	0.38577				
	91 -> 95	0.11493				
Excited State	15:	Singlet-A	4.2449 eV	292.08 nm	f=0.1776	<S**2>=0.000
	82 -> 92	-0.22997				
	83 -> 92	0.10373				
	85 -> 92	0.25929				
	86 -> 92	-0.10436				
	88 -> 93	0.20337				
	88 -> 94	-0.11943				
	89 -> 93	0.44518				
	90 -> 93	-0.10628				
	90 -> 94	0.18293				
	91 -> 95	-0.14608				
Excited State	16:	Singlet-A	4.2721 eV	290.22 nm	f=0.0155	<S**2>=0.000
	88 -> 93	0.11772				
	88 -> 94	0.55943				
	88 -> 95	0.17552				
	89 -> 93	0.20217				
	89 -> 94	-0.14389				
	90 -> 94	-0.19889				
Excited State	17:	Singlet-A	4.4317 eV	279.76 nm	f=0.0137	<S**2>=0.000
	82 -> 92	0.39401				
	83 -> 92	0.12846				

(Continued)

84 -> 92	0.24459
85 -> 92	0.44410
88 -> 95	-0.10528
90 -> 95	-0.11359
Excited State 18:	Singlet-A 4.4333 eV 279.67 nm f=0.0523 <S**2>=0.000
82 -> 92	0.13408
88 -> 94	-0.21188
88 -> 95	0.50050
88 -> 96	0.18808
89 -> 94	0.12826
89 -> 95	-0.12158
90 -> 95	0.24345
Excited State 19:	Singlet-A 4.5330 eV 273.52 nm f=0.0052 <S**2>=0.000
81 -> 92	0.13556
87 -> 94	0.14802
88 -> 94	0.17131
89 -> 94	0.61899
90 -> 95	-0.13155
91 -> 94	-0.10395
Excited State 20:	Singlet-A 4.6026 eV 269.38 nm f=0.0133 <S**2>=0.000
87 -> 95	-0.18076
88 -> 95	-0.26453
88 -> 96	-0.11436
89 -> 94	0.10311
90 -> 95	0.50890
90 -> 96	0.19007
Excited State 21:	Singlet-A 4.6418 eV 267.11 nm f=0.0143 <S**2>=0.000
80 -> 92	-0.13985
83 -> 92	0.62939
84 -> 92	-0.17661
85 -> 92	-0.17665
Excited State 22:	Singlet-A 4.7040 eV 263.57 nm f=0.0086 <S**2>=0.000

(Continued)

80 -> 92	-0.37460
82 -> 92	-0.13094
82 -> 94	-0.13706
84 -> 92	0.11586
86 -> 94	0.44620
87 -> 94	-0.17033
89 -> 94	0.12718
Excited State 23:	Singlet-A 4.7339 eV 261.91 nm f=0.2128 <S**2>=0.000
80 -> 92	0.11545
81 -> 92	-0.18106
85 -> 93	-0.15747
87 -> 93	-0.21608
91 -> 95	-0.20680
91 -> 96	0.52458
Excited State 24:	Singlet-A 4.7871 eV 259.00 nm f=0.4339 <S**2>=0.000
80 -> 92	-0.14983
81 -> 92	0.58223
87 -> 94	0.13795
89 -> 94	-0.15464
90 -> 94	0.12231
91 -> 96	0.17504
Excited State 25:	Singlet-A 4.8237 eV 257.03 nm f=0.0198 <S**2>=0.000
80 -> 92	0.50883
81 -> 92	0.10554
82 -> 92	0.11178
82 -> 94	-0.18444
86 -> 94	0.36781
87 -> 94	-0.10788
Excited State 26:	Singlet-A 4.9024 eV 252.90 nm f=0.0093 <S**2>=0.000
87 -> 93	0.62746
91 -> 95	-0.12183
91 -> 96	0.21821
91 -> 97	0.10215

(Continued)

Excited State	27:	Singlet-A	4.9832 eV	248.80 nm	f=0.0326	<S**2>=0.000
	82 -> 93	0.16970				
	84 -> 93	0.26528				
	85 -> 93	-0.21952				
	86 -> 93	0.55233				
	91 -> 97	-0.10470				
Excited State	28:	Singlet-A	5.0395 eV	246.02 nm	f=0.0118	<S**2>=0.000
	82 -> 95	0.16089				
	84 -> 95	0.14194				
	85 -> 93	0.12270				
	86 -> 95	0.18908				
	87 -> 94	-0.10373				
	87 -> 95	-0.15960				
	89 -> 95	-0.17817				
	91 -> 96	0.12164				
	91 -> 97	0.47335				
Excited State	29:	Singlet-A	5.0678 eV	244.65 nm	f=0.0143	<S**2>=0.000
	82 -> 94	-0.11493				
	82 -> 95	-0.20385				
	84 -> 95	-0.16514				
	85 -> 93	0.10189				
	85 -> 95	0.10666				
	86 -> 93	0.12010				
	86 -> 95	-0.26782				
	86 -> 96	-0.11561				
	87 -> 95	0.16615				
	89 -> 95	0.15549				
	90 -> 96	0.10173				
	91 -> 97	0.37953				
Excited State	30:	Singlet-A	5.1331 eV	241.54 nm	f=0.0378	<S**2>=0.000
	80 -> 94	0.14148				
	81 -> 92	-0.10581				
	82 -> 94	-0.21161				
	83 -> 94	0.16337				

(Continued)

84 -> 93	0.13951
84 -> 94	0.51109
85 -> 94	-0.13394
87 -> 94	0.19280

Table S8 Computed vertical excitations of Pt-py.

Excited State 1:	Singlet-A	3.1308 eV	396.01 nm	f=0.0210	<S**2>=0.000
91 -> 92	0.68483				
Excited State 2:	Singlet-A	3.5047 eV	353.76 nm	f=0.1297	<S**2>=0.000
88 -> 92	-0.28857				
89 -> 92	-0.30656				
90 -> 92	0.55005				
Excited State 3:	Singlet-A	3.5268 eV	351.54 nm	f=0.3346	<S**2>=0.000
90 -> 92	0.12118				
91 -> 93	0.67424				
Excited State 4:	Singlet-A	3.6013 eV	344.27 nm	f=0.1967	<S**2>=0.000
88 -> 92	0.38649				
89 -> 92	0.40816				
90 -> 92	0.39986				
91 -> 93	-0.10092				
Excited State 5:	Singlet-A	3.9137 eV	316.79 nm	f=0.2276	<S**2>=0.000
87 -> 92	0.12514				
88 -> 92	0.48643				
89 -> 92	-0.46404				
91 -> 92	-0.10979				
Excited State 6:	Singlet-A	3.9836 eV	311.23 nm	f=0.0481	<S**2>=0.000
88 -> 93	-0.29336				
89 -> 93	-0.30475				
90 -> 93	0.54286				

(Continued)

Excited State	7:	Singlet-A	4.0017 eV	309.83 nm	f=0.0173	<S**2>=0.000
	88 -> 93	0.14746				
	89 -> 93	0.16284				
	91 -> 94	0.57544				
	91 -> 95	0.23122				
	91 -> 96	0.15585				
Excited State	8:	Singlet-A	4.0841 eV	303.58 nm	f=0.0541	<S**2>=0.000
	88 -> 93	0.32811				
	89 -> 93	0.37892				
	90 -> 93	0.41661				
	91 -> 94	-0.21103				
Excited State	9:	Singlet-A	4.2304 eV	293.08 nm	f=0.0121	<S**2>=0.000
	86 -> 92	-0.21041				
	89 -> 93	-0.10605				
	89 -> 95	-0.12250				
	91 -> 94	-0.28257				
	91 -> 95	0.43280				
	91 -> 96	0.31507				
Excited State	10:	Singlet-A	4.2581 eV	291.17 nm	f=0.2609	<S**2>=0.000
	85 -> 92	0.11793				
	86 -> 92	-0.33456				
	87 -> 92	0.18260				
	88 -> 93	0.36550				
	89 -> 93	-0.29228				
	91 -> 94	0.10643				
	91 -> 95	-0.15326				
	91 -> 96	-0.11135				
Excited State	11:	Singlet-A	4.2707 eV	290.31 nm	f=0.1694	<S**2>=0.000
	85 -> 92	-0.15384				
	86 -> 92	0.44576				
	87 -> 92	-0.14622				
	88 -> 93	0.29719				
	89 -> 93	-0.32943				

(Continued)

Excited State	12:	Singlet-A	4.3434 eV	285.45 nm	f=0.0051	<S**2>=0.000
	88 -> 93	-0.17542				
	88 -> 94	-0.21602				
	88 -> 95	-0.17755				
	88 -> 96	-0.13374				
	89 -> 94	-0.23754				
	89 -> 95	-0.21308				
	89 -> 96	-0.15705				
	90 -> 94	0.35547				
	90 -> 95	0.22018				
	90 -> 96	0.14768				
Excited State	13:	Singlet-A	4.3822 eV	282.93 nm	f=0.0130	<S**2>=0.000
	87 -> 94	0.10537				
	88 -> 94	0.17767				
	88 -> 95	0.21319				
	88 -> 96	0.16732				
	89 -> 94	0.14494				
	89 -> 95	0.18750				
	89 -> 96	0.14495				
	90 -> 94	0.49923				
Excited State	14:	Singlet-A	4.4639 eV	277.75 nm	f=0.0416	<S**2>=0.000
	85 -> 92	-0.22304				
	86 -> 92	0.14626				
	87 -> 92	0.59427				
Excited State	15:	Singlet-A	4.4949 eV	275.83 nm	f=0.0011	<S**2>=0.000
	83 -> 92	0.11119				
	84 -> 92	0.38904				
	85 -> 92	0.44597				
	86 -> 92	0.24486				
	87 -> 92	0.16928				
Excited State	16:	Singlet-A	4.5665 eV	271.51 nm	f=0.0302	<S**2>=0.000
	88 -> 94	0.33062				
	88 -> 95	-0.12454				

(Continued)

89 -> 94	0.33668
89 -> 95	-0.16797
89 -> 96	-0.11121
90 -> 94	-0.14170
90 -> 95	0.31292
90 -> 96	0.22987
Excited State 17:	Singlet-A 4.6319 eV 267.67 nm f=0.0741 <S**2>=0.000
87 -> 95	0.10042
87 -> 96	0.10644
88 -> 94	-0.14062
88 -> 95	0.19813
88 -> 96	0.15950
89 -> 94	-0.24671
89 -> 95	0.14691
89 -> 96	0.10299
90 -> 94	-0.22527
90 -> 95	0.30762
90 -> 96	0.24130
91 -> 96	0.18417
Excited State 18:	Singlet-A 4.7023 eV 263.67 nm f=0.2498 <S**2>=0.000
84 -> 92	0.22394
85 -> 92	-0.11563
85 -> 93	0.12482
87 -> 93	-0.13979
88 -> 95	-0.11055
89 -> 95	-0.12041
90 -> 95	-0.10798
91 -> 95	-0.32061
91 -> 96	0.41199
Excited State 19:	Singlet-A 4.7871 eV 259.00 nm f=0.0038 <S**2>=0.000
82 -> 92	0.15876
87 -> 93	0.16626
87 -> 94	0.15104
88 -> 94	0.43472

(Continued)

89 -> 94	-0.42743
91 -> 94	-0.10768
Excited State 20:	Singlet-A 4.8340 eV 256.49 nm f=0.0581 <S**2>=0.000
83 -> 92	0.17065
84 -> 92	0.38100
85 -> 92	-0.32311
87 -> 93	0.36176
88 -> 94	-0.11595
91 -> 95	0.10307
91 -> 96	-0.10628
Excited State 21:	Singlet-A 4.8747 eV 254.34 nm f=0.0352 <S**2>=0.000
84 -> 92	-0.20340
85 -> 92	0.11158
86 -> 93	-0.12497
87 -> 93	0.47944
91 -> 95	-0.21070
91 -> 96	0.24715
91 -> 97	0.17483
Excited State 22:	Singlet-A 4.9412 eV 250.92 nm f=0.0063 <S**2>=0.000
81 -> 92	-0.26096
84 -> 93	0.23298
85 -> 92	0.11881
85 -> 93	0.16619
86 -> 93	0.50531
87 -> 93	0.14393
Excited State 23:	Singlet-A 5.0004 eV 247.95 nm f=0.0173 <S**2>=0.000
81 -> 92	-0.24939
82 -> 92	-0.14274
84 -> 95	0.12567
85 -> 93	-0.22185
86 -> 93	-0.15575
86 -> 94	0.20775
86 -> 95	0.18237

(Continued)

86 -> 96	0.16647
87 -> 94	-0.11138
91 -> 97	0.31447
Excited State 24:	Singlet-A 5.0051 eV 247.71 nm f=0.3105 <S**2>=0.000
82 -> 92	0.45847
83 -> 92	0.34992
87 -> 94	0.13307
88 -> 94	-0.16589
90 -> 94	-0.13234
Excited State 25:	Singlet-A 5.0343 eV 246.28 nm f=0.0152 <S**2>=0.000
81 -> 92	0.12304
83 -> 92	0.16389
84 -> 93	0.15419
84 -> 96	-0.10181
86 -> 94	-0.16429
86 -> 95	-0.17174
86 -> 96	-0.13691
87 -> 93	-0.12562
91 -> 97	0.49574
Excited State 26:	Singlet-A 5.0739 eV 244.36 nm f=0.0048 <S**2>=0.000
81 -> 92	0.32767
82 -> 92	0.19443
83 -> 92	-0.27517
84 -> 92	0.12362
84 -> 95	0.12035
85 -> 92	-0.10803
85 -> 93	0.21000
86 -> 95	0.17945
86 -> 96	0.14079
91 -> 97	0.13554
Excited State 27:	Singlet-A 5.1162 eV 242.34 nm f=0.0049 <S**2>=0.000
81 -> 92	0.27169
82 -> 92	-0.29755

(Continued)

83 -> 92	0.38697
84 -> 92	-0.17505
84 -> 93	0.15966
85 -> 93	0.15225
90 -> 96	0.11450
Excited State 28:	Singlet-A 5.1590 eV 240.33 nm f=0.0969 <S**2>=0.000
88 -> 95	0.26679
88 -> 96	-0.21331
89 -> 95	0.13802
89 -> 96	-0.31639
90 -> 95	-0.26440
90 -> 96	0.33569
91 -> 97	0.11212
Excited State 29:	Singlet-A 5.1943 eV 238.69 nm f=0.0107 <S**2>=0.000
81 -> 92	-0.22765
81 -> 93	-0.17055
85 -> 93	0.44374
86 -> 93	-0.26139
88 -> 95	0.14052
89 -> 95	-0.15967
90 -> 95	0.10431
90 -> 96	-0.19526
Excited State 30:	Singlet-A 5.2131 eV 237.83 nm f=0.0371 <S**2>=0.000
81 -> 92	-0.19560
83 -> 92	-0.14313
83 -> 93	0.12081
84 -> 93	0.40496
86 -> 93	-0.23730
88 -> 95	-0.24100
89 -> 95	0.16941
91 -> 96	0.11487
91 -> 99	-0.12868

References.

- S1 M. Kimura, M. Yoshida, S. Fujii, A. Miura, K. Ueno, Y. Shigeta, A. Kobayashi and M. Kato, *Chem. Commun.*, 2020, **56**, 12989–12992.